Available online at www.sciencedirect.com

ScienceDirect

Procedia Structural Integrity 81 (2026) 327–332

Structural Integrity Procedia

www.elsevier.com/locate/procedia

VIII International Conference "In-service Damage of Materials: Diagnostics and Prediction"(DMDP 2025)

Study of low-cycle fatigue of concrete bonding to sickle-shaped reinforcement

Oleksandr Chapiuk*, Olha Homon, Olena Pakholiuk, Svitlana Rotko, Vladislav Volyansky, Volodymyr Samchuk, Oleksandr Andriichuk, Alla Martyniuk

Lutsk National Technical University, Lvivska 75, 43018 Lutsk, Ukraine

Abstract

The definition of low-cycle bond fatigue between concrete and reinforcing bars is presented. It has been experimentally established that low-cycle bond fatigue of reinforcement in concrete under high-level cyclic loading occurs during the elastic-plastic slip of the reinforcing bars. Furthermore, a formula is proposed to describe the low-cycle bond fatigue of concrete with deformed bars. This formula shows good agreement with experimental data; for the materials investigated, the relative low-cycle endurance value constitutes 0.88.

© 2026 The Authors. Copy from the contract: Published by ELSEVIER B.V.
This is an open access article under the CC BY-NC-ND license (https://creativecommons.org/licenses/by-nc-nd/4.0)
Peer-review under responsibility of DMDP 2025 organizers

Keywords: bond between concrete and reinforcement; bond stress; sickle-shaped profile; bond fatigue; reinforcement deformations; cyclic loading.

1. Introduction

Ensuring the reliability and long-term service life of buildings and structures are priority tasks in the construction industry (Parneta et al. (2024); Filipchuk et al. (2023); Babich et al. (2019);)). Various materials are used in their construction (Mel'nyk et al. (2019); Rybak et al. (2025)). Concrete and reinforced concrete structures are the most widely used in construction practice (Konkol et al. (2022); Chapiuk et al. (2025); Dvorkin et al. (2021); Sobczak-Piastka et al. (2020)). The bond between reinforcement and concrete is a determining factor in ensuring their composite action within reinforced concrete structures (Chapiuk et al. (2025)). The vast majority of structures are subjected to repeated low-cycle loading, which can affect the mechanical characteristics of the materials. Only isolated studies have been devoted to these issues (Babych et al. (2017); Dovbenko et al. (2024); Filipchuk et al. (2024); Drobyshynets et al. (2024)). Recently, sickle-shaped reinforcement has been used in reinforced concrete; its bond with concrete has been insufficiently investigated (DSTU 3760:2019, DBN B.1.2-14-2018; Eurocode 2 (2004)), and under the action of repeated low-cycle loading, it has hardly been examined at all.

Therefore, investigating the bond characteristics of sickle-shaped reinforcement with concrete is a crucial task, particularly in relation to its low-cycle fatigue properties. In general, the concept of low-cycle bond fatigue between reinforcement and concrete

* Corresponding author. Tel.: +38-099-227-19-87.
E-mail address: ochapiuk1983@gmail.com

2452-3216 © 2026 The Authors. Copy from the contract: Published by ELSEVIER B.V.
This is an open access article under the CC BY-NC-ND license (https://creativecommons.org/licenses/by-nc-nd/4.0)
Peer-review under responsibility of DMDP 2025 organizers
10.1016/j.prostr.2026.03.057

is currently scarcely addressed in either technical or regulatory literature. Low-cycle fatigue of materials is defined as fatigue in which failure or damage occurs under conditions of elastic-plastic deformation (Korniychuck et al. (2024); Kos et al. (2019); Kovalchuk et al. (2022)). Consequently, in this context, low-cycle bond fatigue between the reinforcement and concrete is understood as fatigue failure that occurs during the elastic-plastic slip of the reinforcing bar within the concrete. The low-cycle endurance limit is taken as the maximum absolute bond stress at which fatigue failure does not yet occur. This phenomenon typically arises under repeated loading at high levels of bond stress between the concrete and the reinforcing bars.

High-cycle fatigue occurs when fatigue damage or failure takes place primarily under elastic deformation. The boundary between low-cycle and high-cycle fatigue is somewhat arbitrary.

In view of this, experimental studies were conducted on the low-cycle bond fatigue of class A500C sickle-shaped reinforcement in concrete, the analysis of which is presented below.

Nomenclature

f_{cube}	cubic strength of concrete
f_{prism}	prismatic strength of concrete
σ_u	temporary tensile strength of rods
E_s	initial modulus of elasticity of reinforcement
A_s	area of rods
d	reinforcement diameter
P	load
δ_u	slip (displacement) of the free end of the rod relative to the end of the prisms
σ_{s0m}	stress in the rod at δ_u=0.2 mm
η	loading level
$\sigma_{0,2}$	0.2% proof stress of reinforcement
η_{cyc}	cycling loading level
σ_s	stress in the rod (beginning of slippage)
υ	coefficient of variation
τ_{um}	tangential stresses
l_{an}	length of rod anchoring in concrete
k	empirical coefficient (16.5 MPa/cm)
R_{sn}	standard tensile strength of reinforcemen
R_s	calculated tensile strength of reinforcement
P_s	level of repeated low-cycle loading

2. Methods of experimental research

As part of the comprehensive investigation into the bond between concrete and sickle-shaped reinforcement, fatigue behavior was studied using specimens fabricated as concrete prisms with a 150 mm square cross-section. The height of the concrete prisms was determined by the adopted anchorage length, which was set at 5d (where d = 16 mm is the diameter of the bar), i.e., 80 mm. The reinforcing bars were positioned within the prisms such that their longitudinal axes coincided. The protruding ends of the bars were designed to allow clamping in the testing machine grips on one side, and measurement of the displacement (slip) relative to the concrete prism face on the other (free) side (Fig. 1).

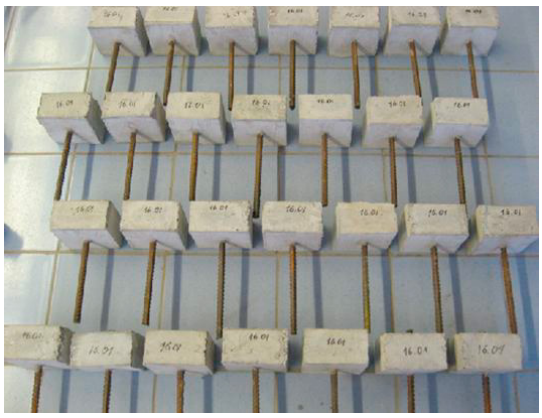

Fig. 1. General view of the specimens.

The specimens were fabricated using class C20/25 concrete, which exhibited a 28-day cube compressive strength of f_{cube} = 32 MPa and a prism compressive strength of f_{prism} = 23.7 MPa at the commencement of testing of the main specimens. Class A500C reinforcement was used, characterized by the following mechanical properties: ultimate tensile strength σ_u = 675 MPa; 0.2% proof stress $\sigma_{0.2}$ = 498 MPa; and modulus of elasticity E_s = 200000 MPa.

In accordance with British Standard BS 4449:1997, the limit state of the bond between reinforcement and concrete is defined as the condition where the slip of the free end of the bar relative to the prism face reaches δ_u= 0.2 mm. Consequently, this value of δ_u corresponds to the reinforcement stress σ_{s0}.

The investigation of the bond between reinforcement and concrete was performed through pull-out tests, in which metal bars were extracted from concrete prisms using a specialized tensioning device mounted in a hydraulic tensile testing machine (Fig. 2a). The load was applied to the bar in increments of 1.0 kN, with a 3-minute dwell time maintained at each loading level (note: the specific 3-minute duration is from your query and is not explicitly mentioned in the sources). During loading, the slip of the free end of the bar relative to the prism face was measured using a dial gauge with a 0.001 mm division, while bar deformations at the loaded end were measured using a Huggenberger extensometer (20 mm gauge length, 0.001 mm division).

Six specimens were tested to determine the reinforcement stress σ_{s0} under monotonic loading to failure (Fig. 2b). Subsequent specimens were subjected to cyclic loading at relative levels $\eta_{cyc} = \sigma_{s,cyc}/\sigma_{s0}$ of 0.98, 0.95, 0.93, and 0.91. The cyclic loading was applied to the respective relative levels, followed by complete unloading to zero, and these cycles were repeated until the bar slip reached the limiting value of $\delta_{u,cyc}$ = 0.2 mm. In the specimen designation system, the first digit indicates the applied cyclic loading level, and the second digit represents the specimen number. The letters "k" and "p" indicate that the specimens were tested under short-term monotonic and cyclic loading, respectively.

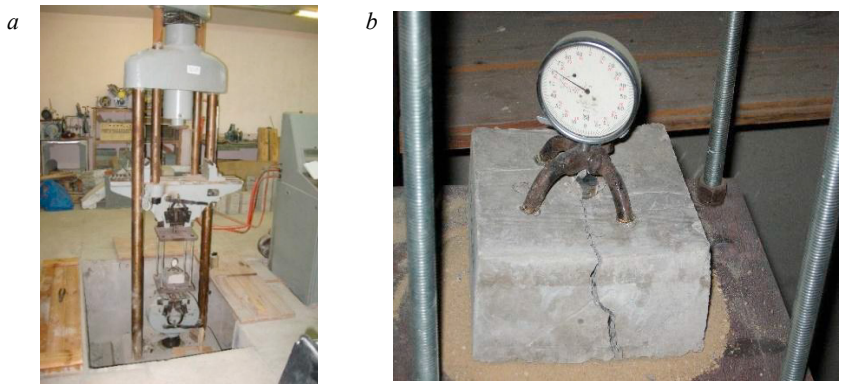

Fig. 2. General view of the test setup (a); and failure mode of the specimens (b).

3. Results and discussion

Based on the test results of six specimens (P-1k through P-6k), it was determined that under monotonic loading to failure, the mean stress in the reinforcing bars corresponding to a slip of δ_u= 0.2 mm was σ_{s0} = 135 MPa. All six specimens exhibited consistent behavior under loading; the standard deviation of the stress values was σ = 3.2 MPa, with a coefficient of variation of υ = 0.024. Therefore, the adopted baseline stress value σ_{s0} is statistically justified.

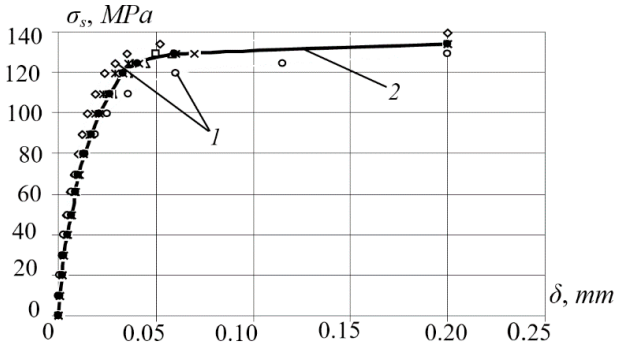

Fig. 3. Bar slip under monotonic loading versus reinforcement stress (1 – experimental values; 2 – mean values from testing six identical specimens P-1…6k).

The subsequent specimens were subjected to cyclic loading, in which the maximum reinforcement stress level was defined as a fraction of the baseline stress, i.e., $\sigma_{s,cyc} = \eta_{cyc}\sigma_{s0}$. Cyclic loading was applied until the bar slip in each specimen reached $\delta_{u,cyc} = 0.2$ mm. $\sigma_{s0,\,cyc}$ represents the stress $\sigma_{s,cyc}$ corresponding to the attainment of the limiting slip value, and $n_{u,cyc}$ denotes the number of cycles sustained by the specimen prior to reaching the limit state.

For four specimens (P-1p/0.98 through P-4p/0.98), the cyclic loading level was set to $\eta_{cyc} = 0.98$. Two specimens reached the limit state on the second cycle, while the other two reached it on the third and fourth cycles, respectively. In specimen P-3p/0.98, under a stress of $\sigma_{s,\,cyc} = 132$ MPa, the bar slip values on the first and second cycles were $\delta_{cyc} = 0.093$ mm and 0.125 mm, respectively; on the third cycle, the slip reached $\delta_{u,\,cyc} = 0.2$ mm (Fig. 4a). For specimen P-4p/0.98, the bar slip gradually increased during the first, second, and third cycles, amounting to $\delta_{cyc} = 0.080$, 0.107, and 0.134 mm, respectively, before reaching $\delta_{u,\,cyc} = 0.2$ mm on the fourth cycle. Thus, it can be concluded that at $\eta_{u,\,cyc} = 0.98$, fatigue failure occurred between the 2nd and 4th cycles for these specimens (where $\eta_{u,\,cyc} = \eta_{cyc}$ at the failure cycle).

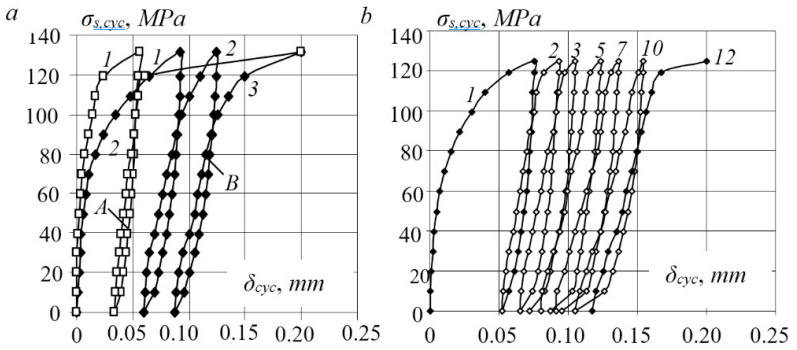

Fig. 4. Bar slip under cyclic loading: (a) in specimens P-2p/0.98 (A) and P-3p/0.98 (B); (b) in specimen P-10p/0.93 (numbers indicate loading cycles).

At a loading level of $\eta_{cyc} = 0.95$, two specimens sustained three cycles each, while one specimen sustained seven cycles. In specimen P-7p/0.95, under a stress of $\sigma_{s,cyc} = 128$ MPa, the total bar slip progressively increased from cycle to cycle. While the slip was $\delta_{cyc} = 0.075$ mm in the first cycle, it increased to 0.093, 0.115, 0.160, and 0.185 mm in the second, third, fifth, and sixth cycles, respectively.

On the seventh cycle, the slip reached its limiting value. It should be noted that a gradual increase in residual slip deformations was observed during the loading cycles, indicating that fatigue failure occurred during the elastic-plastic slip of the reinforcing bar.

In the following specimens, the cyclic loading level was reduced to $\eta_{cyc} = 0.93$, resulting in an increased number of cycles to fatigue failure compared to the previous specimens. Specimens P-8p/0.93, P-9p/0.93, and P-10p/0.93 reached the limit state at the ninth, tenth, and twelfth cycles, respectively. In all specimens prior to this state, elastic-plastic slip of the bars was observed.

In specimen P-10p/0.93 (see Fig. 4b), which failed on the 12th cycle, the total bar slip on the 10th and 11th cycles was $\delta_{cyc} = 0.154$ and 0.162 mm, respectively, representing 77% and 81% of the limiting value reached on the 12th cycle. An increase in residual slip was also observed up to the final cycle, amounting to 55% of the maximum value on the 11th cycle. In this instance, the slip increment was 0.005 mm, which is significantly less than in specimen P-7p/0.95, where the residual slip increment on the penultimate cycle was 0.027 mm. This indicates that a further reduction in the cyclic loading level will approach the low-cycle endurance limit.

For specimens P-11p/0.91, P-12p/0.91, and P-13p/0.91, the cyclic loading level was reduced to $\eta_{cyc} = 0.91$ ($\eta_{cyc} = 0{,}91$ ($\sigma_{s,cyc} = 122.5$ MPa)). This resulted in an increase in the number of cycles to fatigue failure, with the specimens sustaining 35, 41, and 44 cycles, respectively (Fig. 5).

In specimen P-12p/0.91, over the first five cycles, the total slip increased from $\delta_{cyc} = 0.048$ mm in the first cycle to $\delta_{cyc} = 0.081$ mm in the fifth. Subsequently, the slip gradually increased, changing from 0.136 mm to 0.151 mm between the 20th and 25th cycles. That is, by the 25th cycle, the slip amounted to 75.5% of the limiting value. From the 35th to the 40th cycle, the slip increased monotonically, reaching $\delta_{cyc} = 0.199$ mm on the 40th cycle, which is practically equal to the limiting value; however, the specimen continued to function until the 41st cycle, at which point failure occurred (see Fig. 5).

The analysis of the residual bar slip is noteworthy; after the first loading cycle, it amounted to 0.026 mm, representing 13% of the limiting value $\delta_{cyc} = 0.2$ mm. By the 25th cycle, the residual slip had increased to 0.117 mm (58.5% of the limit), and by the 40th cycle, to 0.159 mm (79.5% of the limit). The short-term total slip values observed during loading decreased slightly after the first cycle, subsequently stabilized by the 11th cycle, and remained constant until failure. However, the proportion of plastic slip within these deformations continuously increased.

The residual slip increment decreased as the number of cycles increased, amounting to 0.003 mm between the 38th and 40th cycles, which is lower than that observed in the specimens with $\eta_{cyc} = 0.93$. Thus, although the specimens with $\eta_{cyc} = 0.91$ experienced low-cycle fatigue, they were approaching the high-cycle endurance limit.

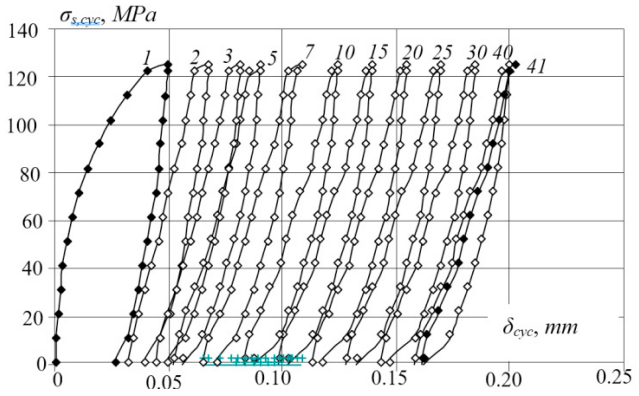

Fig. 5. Bar slip in specimen P-12p/0.91 (numbers indicate loading cycles).

The obtained experimental data enable the establishment of a relationship between the low-cycle endurance level $\eta_{u,\,cyc}$ and the number of cycles to low-cycle fatigue failure $n_{u,\,cyc}$ for the investigated materials (Fig. 6). To describe this relationship, a formula is proposed in the form of Equation (1):

$$\eta_{u,cyc} = 1 - a\frac{n_{u,cyc}-1}{n_{u,cyc}+b}, \tag{1}$$

where a and b are coefficients determined through statistical analysis.

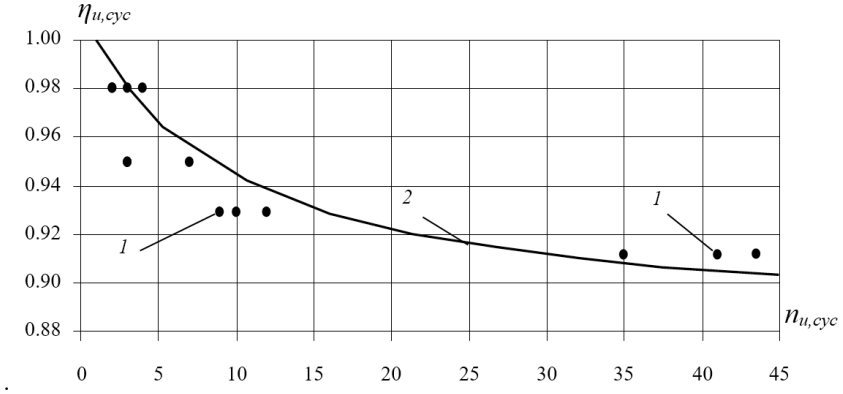

Fig. 6. Low-cycle bond fatigue of reinforcement in concrete: 1 – experimental points; 2 – theoretical curve according to Eq. (1).

The coefficients a and b are determined based on the least squares minimization of the deviation between the experimental and theoretical curves. Under the conditions of the performed experiment, the coefficient values were found to be $a = 0.12$ and $b = 8.5$. Using these coefficient values, the theoretical relative low-cycle endurance levels, $\eta_{u,\,cyc,th}$ were calculated via Eq. (1) for the corresponding experimental cycle values $n_{u,\,cyc}$. The mean ratio of experimental to theoretical values ($n_{u,\,cyc}/\eta_{u,\,cyc,th}$) is 0.993, with a standard deviation of $\sigma = 0.013$ and a coefficient of variation of $\upsilon = 0.013$ (1.3%). These statistical metrics indicate that Eq. (1) provides an accurate description of the low-cycle bond fatigue between concrete and sickle-shaped reinforcing bars.

According to Eq. (1), as $n_{u,\,cyc} \to \infty$, the low-cycle endurance limit amounts to $\eta_{u,\,cyc} = 0.88$. Given that low-cycle fatigue occurs during the elastic-plastic slip of the bars, it is likely necessary to conduct further experiments with concretes of various strength classes, which exhibit different elastic-plastic characteristics, to refine the value of $\eta_{u,\,cyc}$.

4. Conclusions

The definition of the concept of low-cycle bond fatigue between concrete and reinforcing bars is presented. It has been experimentally established that low-cycle bond fatigue between reinforcement and concrete under high-level cyclic loading occurs during the elastic-plastic slip of the reinforcing bars within the concrete. A formula is proposed to describe the low-cycle bond fatigue of concrete with deformed bars, which demonstrates good agreement with the experimental data. For the materials

investigated, the relative low-cycle endurance value constitutes 0.88. For other concrete strength classes and reinforcement diameters, additional experimental research is necessary to refine the empirical coefficients.

References

Babich, Y., Filipchuk, S., Karavan, V., Sobczak-Piastka, J., 2019. Research of basic mechanical and deformative properties of high-strength fast-hardening concretes. AIP Conference Proceedings 2077, 020003.

Babych, Y.M., Savitskiy, V.V., Andriichuk, O.V., Ninichuk, M.V., Kysliuk, D.Y., 2019. Results of experimental research of deformability and crack-resistance of two span continuous reinforced concrete beams with combined reinforcement. IOP Conference Series: Materials Science and Engineering 708(1), 012043.

BRITISH STANDARD BS 4449: 1997. Specification for carbon steel bars for the reinforcement of concrete.

Chapiuk, O., Kratiuk, O., Zadorozhnikova, I., Boiarska, I., Rud, V., Boiarskyi, M., Mudryy, I., Pelekh, A., 2025. Method for determining the minimum anchorage length of reinforcement in concrete: an experimental study. Procedia Structural Integrity 72, 308–314.

Chapiuk, O., Oreshkin, D., Hryshkova, A., Pakholiuk, O., Avramenko, Y., 2023. Adhesion of the metal and composite fiberglass rebar with the heavyweight concrete. Lecture Notes in Civil Engineering 299, 47–60.

Drobyshynets, S., Babych, Y., Sunak, P., Zadorozhnikova, I., Parfentyeva, I., Pakharenko, V., Homon, S., 2024. Experimental and theoretical studies of fatigue of steel fibre reinforced concrete under low-cycle compression. Procedia Structural Integrity 59, 601–608.

DSTU 3760:2019, 2019. Prokat armaturnyy dlya zalizobetonnykh konstruktsiy. Zahal′ni tekhnichni umovy [Reinforcing bars for reinforced concrete structures. General technical conditions]. Ministry of Regional Development of Ukraine, Kyiv, 18 p.

Dovbenko, V., Kukhniuk, O., Homon, S., Ivaniuk, A., Aleksiievets, V., Savytska, O., Kulakovskyi, L., 2024. Study of the strength properties of concrete impregnated with a polymer composition. Procedia Structural Integrity 59, 702–709.

Dvorkin, L., Bordiuzhenko, O., Zhitkovsky, V., Gomon, S., Homon, S., 2021. Mechanical properties and design of concrete with hybrid steel basalt fiber. E3S Web of Conferences 264, 02030.

Eurocode 2, 2004. Design of concrete structures – Part 1-1: General rules and rules for buildings. CEN, Brussels, 225 p.

Filipchuk, S., Karavan, V., Makarenko, R., Nalepa, O., Chapiuk, O., 2023. Study of reinforcement adhesion to concrete under static and dynamic loads. AIP Conference Proceedings 2949, 020007.

Filipchuk, S., Karavan, V., Nalepa, O., Chapiuk, O., Pakholiuk, O., 2024. Stability of slabs made of high-strength concrete subjected to dynamic influence. Procedia Structural Integrity 59, 588–594.

Konkol, J., 2019. Fracture toughness and fracture surface morphology of concretes modified with selected additives of pozzolanic properties. Buildings 9(8), 174.

Korniychuk, O., Masiuk, G., Homon, S., Aleksiievets, I., Chapiuk, O., Kaynts, D., Rizak, V., 2024. Deformability of reinforced concrete beams under the action of repeated alternating loads. Procedia Structural Integrity 59, 575–582.

Kos, Z., Klymenko, Y., Karpiuk, I., Grynyova, I., 2022. Bearing capacity near support areas of continuous reinforced concrete beams and high grillages. Applied Sciences 12(2), 685.

Kovalchuk, V., Rybak, R., Parneta, B., Onyshchenko, A., Kvasnytsya, R., 2022. Determining patterns of the deformed state of the transport concrete pipe reinforced with a metal clamp under the action of static load. Eastern-European Journal of Enterprise Technologies, 5/7 (119), 54–60.

Mel'nyk, I., 2019. Stiffness of monolithic reinforced-concrete slab structures. Materials Science 55(3), 367–373.

Parneta, B., Kovalchuk, V., Rybak, R., 2024. Methodology for evaluating the stress-strain state of strengthened concrete pipe using the finite element method with FEMAP with NX Nastran. Lecture Notes in Civil Engineering 604, 415–425.

RILEM/CEB/FIP Recommendations RC 5, 1978. Bond test for reinforcing steel. 1. Beam test.

Rybak, R., Kovalchuk, V., Parneta, B., 2025. Establishment of regularities in the stress-strain state of strengthened reinforced concrete pipes under force loads and thermal effects. Lecture Notes in Civil Engineering 781, 354–362.

Sobczak-Piastka, J., Babich, Y., Filipchuk, S., Karavan, V., Nalepa, O., 2020. Research of deformative properties of concrete taking into account the descending branch of deformation. IOP Conference Series: Materials Science and Engineering 960(3), 032057.